Paper Nr.: 15

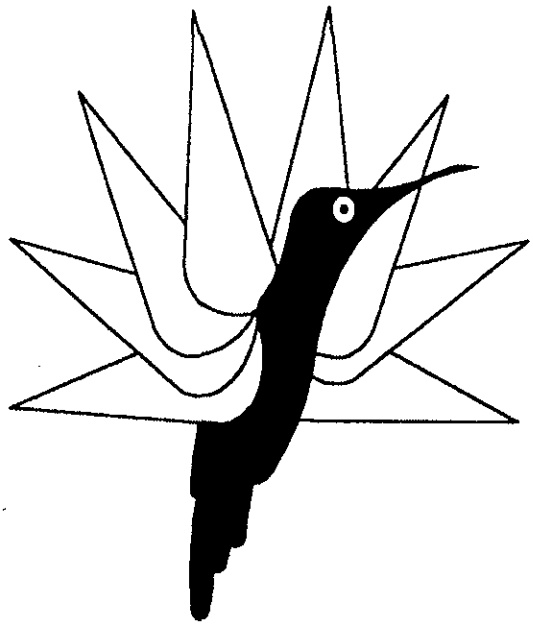

Analysis, Design, and Testing of the Coanda Effect Exhaust Deflector of the V-22 Tiltrotor

By

A.G. Brand, J.L. Jenkins, T.L. Wood

Bell Helicopter Textron Inc.
Fort Worth, Texas

Twentieth European Rotorcraft Forum
October 4-7, 1994 Amsterdam

ABSTRACT

During flight idle operations on the ground, the V-22 engine exhaust impinges on the ground directly below each nacelle. This forces a portion of the hot engine exhaust gases to travel toward the fuselage. Under these conditions various aircraft systems, such as the avionics and APU, are forced to operate in a hot environment. Certain fuselage components are also exposed to elevated temperatures. This condition was resolved during the V-22 Full Scale Development (FSD) program by using a mechanical deflector to direct the hot exhaust gases outboard during ground idle operations. For the Engineering Manufacturing and Development (EMD) phase, a trade study was conducted to optimize the deflector for reduced cost, weight, and complexity. The outcome of the trade study was the selection of a new deflector system that utilizes momentum nozzles and the Coanda effect to direct the exhaust flow away from the fuselage. The nozzles are activated by excess engine bleed air, available during ground operations. Analysis and testing of the system show that the nozzles provide the necessary deflection of exhaust gases. The nozzle system is robust and simple in design, and provides both cost and weight savings for the V-22.

NOMENCLATURE

A	Area, (ft^2))
a	Sound Speed
APU	Auxiliary Power Unit
c	Airfoil Chord, (ft
C_μ	Momentum Coefficient
h	Slot height, (ft)
$\dot{m}$	Mass flow, (slug/s)
M	Mach Number
P_o	Stagnation Pressure
q	Dynamic pressure,(lb/ft^2)
R	Gas Constant for air
S	Airfoil area, (ft^2)
T	Temperature (Absolute)
T_o	Stagnation Temperature
V	Velocity, (ft/s)
ρ	Density, ($slug/ft^3$)
γ	Ratio of specific heats for air –

Subscripts

airfoil	Refers to airfoil data
center	Refers to center nozzle
duct	Refers to ducted flow
exit	Refers to duct exit plane
exhaust	Exhaust conditions
lower	Refers to lower nozzle
s	Refers to slot
slot	Refers to slot conditions
upper	Refers to upper nozzle
∞	Referenced to free stream

INTRODUCTION

The V-22 utilizes a rotor tilting mechanism in which the entire nacelle is pivoted during conversion between helicopter and airplane flight modes. For this design, the engine exhaust flow always complements the rotor thrust. During hover, the exhaust flow alone provides approximately 1500 LB of thrust augmentation. However, during ground operations, this design leads to recirculation of the engine exhaust flow between the V-22 wing and ground as illustrated in Fig. 1.

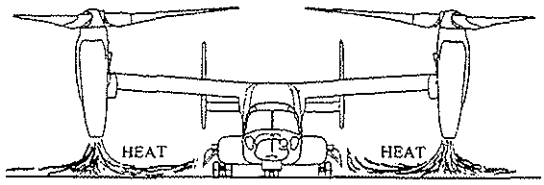

Fig. 1 V-22 exhaust flow during ground operations.

During the V-22 FSD program, a set of mechanically actuated doors were mounted on the end of each engine exhaust nozzle to deflect the hot gases away from the fuselage and ensure an acceptable external temperature environment. A trade study was conducted to optimize this system with the goals of reducing weight, complexity, and cost.

Two approaches were followed in the trade study. One approach was to optimize the mechanical deflector with re-designed lightweight doors and different flow-path geometry. The second approach utilized a concept developed during independent research at Bell helicopter. This approach utilized a system of nozzles, placed at the exhaust exit to deflect the flow using engine bleed air. Use of engine bleed air does not penalize the aircraft performance since the bleed air is used only while on the ground. A maximum of 7% of the primary engine flow could be diverted for exhaust deflection during ground idle operations. This paper focuses on the development of a bleed air deflector system that relies on a momentum and Coanda effect nozzle system to efficiently deflect the exhaust flow.

The Coanda effect, named after the French inventor Henri Coanda, was first discussed in his 1935 patent application (Ref. 1) for a fluid stream deflection device. The effect, now well known in the field of aerodynamics, can be described in part as the ability of a high velocity jet, emerging from an appropriate nozzle into a surrounding fluid, to remain attached to an adjacent curved surface. The jet flow produces a low pressure region on the curved surface which entrains the surrounding fluid to follow, or expand to, the contour of the curved surface. The success of a bleed air deflector system relies on the ability of a high velocity jet stream to promote a lateral momentum to the ducted flow within the constraints of the available bleed air pressure and mass flow rate.

The Coanda effect has been applied variously to control lift on wings (Ref. 2), circulation on rotor blades (Ref. 3), and side force on helicopter tail booms (Ref. 4). In a simplified bleed air deflector system, the Coanda effect is used to deflect a ducted flow as shown in Fig. 2. Two Coanda nozzles are positioned on opposing sides of a ducted flow. When pressure is supplied to the

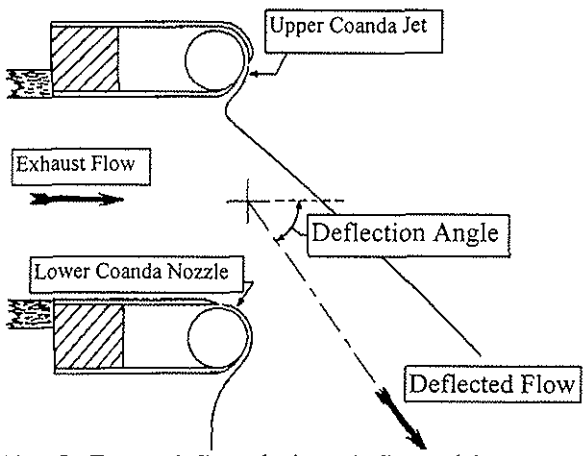

Fig. 2. Ducted flow being deflected by a pair of Coanda effect nozzles.

nozzles a high velocity jet emerges, following the cylindrical contour sketched in Fig. 2 The nozzle flow remains attached in excess of 90 degrees of cylinder arc. Surrounding fluid is entrained, and the ducted flow is effectively deflected from its original trajectory.

Existing literature on circulation control wings provides an indication of the slot flow requirements necessary to substantially deflect the flow. In References 5 and 6, Engler examined the aerodynamic characteristics of airfoils utilizing Coanda effect (circulation control) trailing edges. Variations of nozzle blowing, accomplished by back pressure and slot height changes, were related to the airfoil section lift coefficient. Additional surveys of total pressure in the airfoil wake provided a determination of the amount of flow deflection obtained for a given set of slot conditions. It was shown that high levels of slot blowing could cause the wing wake to impinge on the tunnel floor.

With the airfoil nozzle momentum coefficient, defined as:

$$C_{\mu_{airfoil}} = \frac{\dot{m}_s V_s}{q_\infty \cdot S} = 2 \cdot \frac{\rho_s}{\rho_\infty} \cdot \frac{h}{c} \cdot \left(\frac{V_s}{V_\infty} \right)^2$$

it was found, for a slot height of 0.050 inches and for $C_{\mu_{airfoil}} = 0.467$, that large wing wake deflections could be obtained. Slot mass flows for this operating condition were within the limits of the V-22 engine bleed air capacity. However, the wake deflection for a 2-D airfoil constrained by tunnel walls offers no real information for determining the amount of wake deflection for a ducted flow ejecting into an open atmosphere. To be considered effective, the V-22 exhaust deflector would need to turn the flow approximately 40-45 degrees.

Phase I Proof of Concept Testing

To investigate the ability of bleed air nozzles to deflect a ducted flow, a series of small scale tests were conducted at the BHTI wind generator. The air stream of the wind generator was channeled into a rectangular duct 6.8 inches high by 12 inches wide and vented to the open atmosphere. The upper and lower exit lips of the duct were fitted with Coanda nozzles as shown in Fig. 3.

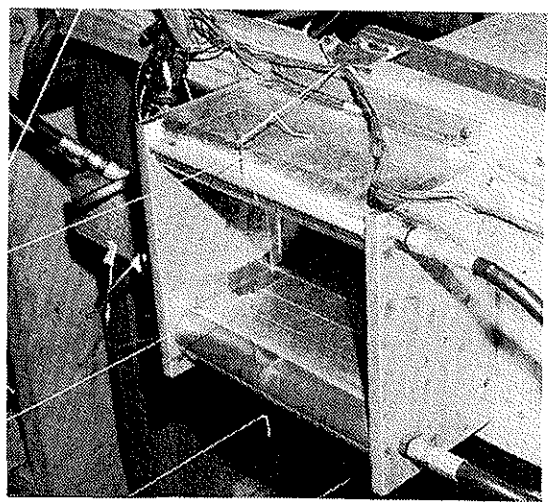

Fig. 3 Ducted flow configured with two Coanda nozzles.

Pressurized air was supplied to the plenums behind each cylinder. Nozzle air was forced through a baffle inside the cylinder and entered the plenum through a series of holes along the plenum/cylinder interface. This allowed a uniform pressure to be developed in the plenum and provided a uniform slot velocity profile. Compressed air storage

bottles, rated at 2500 PSI, provided approximately 6 minutes of run time before plenum pressures (typically operating at 20 inches of water) were affected.

Flow deflection was determined in several ways. A tuft grid, located downstream of the exhaust exit plane gave good indications of flow activity. For visualization, smoke was injected into the duct flow which provided a measure of the wake dispersion angle. Visualization results for the configuration shown in Fig. 3 are shown in Figs. 4a (nozzles off) and 4b (nozzles on). A total pressure survey in the wake

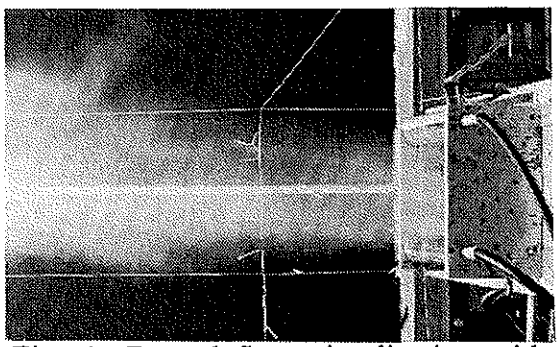

Fig. 4a Ducted flow visualization with Coanda nozzles off.

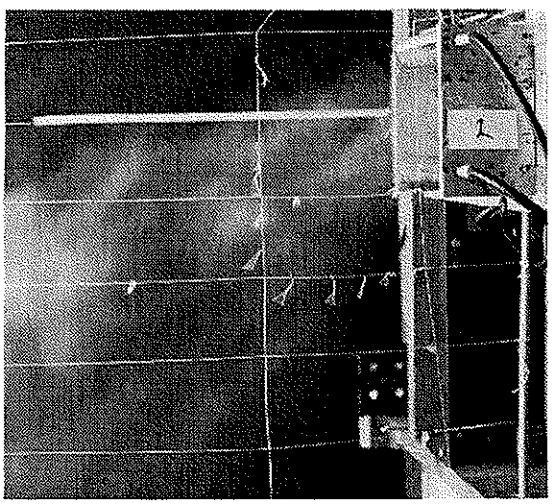

Fig. 4b Coanda Nozzles on.

flow determined that the center of flow was deflected 50 degrees from horizontal for this test condition.Since large flow deflections were obviously possible, it became important to measure the slot operating conditions to determine whether the bleed air requirements would be feasible on a full scale V-22 exhaust.

A modified definition of momentum coefficient was defined for the ducted flow as:

$$C_{\mu_{duct}} = \frac{\left(\dot{m}_s V_s\right)_{upper} + \left(\dot{m}_s V_s\right)_{lower}}{q_{duct} \cdot A_{duct}}$$

$$C_{\mu_{duct}} = 2 \cdot \frac{\sum_{slots} \dot{m}_s V_s}{\dot{m}_{duct} V_{duct}}$$

$$C_{\mu_{duct}} = 2 \cdot \left(\frac{\text{Total Slot Momentum}}{\text{Exhaust Momentum}}\right)$$

To accurately determine the slot mass flow, the compressed air supply bottles were weighed prior to one of the runs. The duct flow was established by setting the tunnel flow, and the compressed air valves were manually opened for a predetermined time interval for each slot and then shut. The air bottles were then re-weighed to determine the mass of air that escaped through the nozzles. Since the time interval and total mass change were known, the average slot mass flow was determined.

Slot velocities were estimated from the measured temperatures and pressures using the isentropic flow relations for compressible flow. By varying the duct (wind tunnel) velocity, the momentum coefficient parameter could be swept

through a range to simulate a variety of operating conditions.

The flow deflection angle versus momentum coefficient is shown in Fig. 5 for a typical test configuration. Data contained in Fig. 5 corresponds to the configuration shown in previous figures. From these results, it is seen that approximately 45 degrees of exhaust flow deflection is obtained for a momentum coefficient approximately equal to 0.4. This indicates that a ducted flow can be deflected significantly using a pair of opposing Coanda effect nozzles operating at C_μ=0.4.

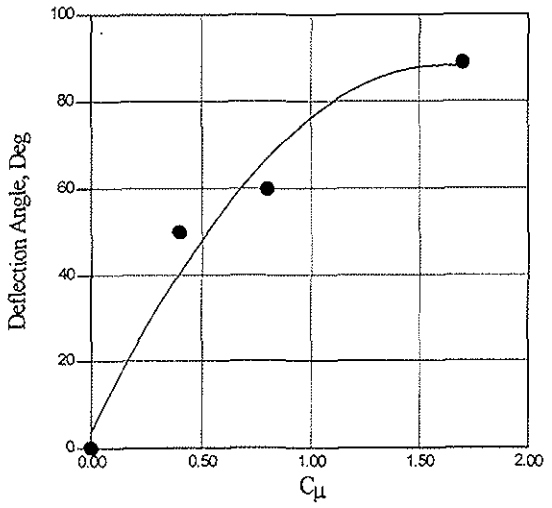

Fig. 5 Coanda Deflector Performance (Phase I Test).

If it is assumed that a bleed air deflector for the V-22 would operate at a similar value of C_μ, it is possible to estimate the minimum required ratio of slot velocity to exhaust velocity. By assuming that each nozzle slot operates at the same conditions, the expression for C_μ may be written as:

$$C_\mu = 2\left(\frac{\dot{m}_{nozzles}}{\dot{m}_{exhaust}}\right)\cdot\left(\frac{V_{slot}}{V_{exhaust}}\right)$$

The maximum value the mass flow ratio for the V-22 engines is 7%. Thus, with C_μ=0.4, the ratio of slot velocity to exhaust flow velocity may be expressed as:

$$\frac{V_{slot}}{V_{exhaust}} = \frac{C_\mu}{2}\left(\frac{\dot{m}_{exhaust}}{\dot{m}_{nozzles}}\right) = 2.85$$

For the V-22 at ground idle conditions, this ratio calls for a subsonic slot velocity that is well within the capability of the bleed air supply to generate. Further wind tunnel tests on a V-22 exhaust configuration were thus warranted.

Phase 2 Wind Tunnel Testing

The engine exhaust flow of the V-22 is essentially comprised of two merging gas streams, which combine at the exhaust duct exit plane. A low velocity region exists in the center of the duct due to the presence of a flow splitting center-body shape. These features of the actual configuration were included in the next phase of wind tunnel testing. For these tests, a 12-inch section of the full scale V-22 exhaust system was installed in the exit plane of the BHTI wind generator.

Since the V-22 exhaust opening is approximately rectangular, the 12-inch wide section approximated a 2-D testing situation, although the end effects are more severe for the short span tested. The model incorporated the full scale height dimensions of the actual exhaust duct (distance between the nozzles) so that the effect of nozzle separation distance could be evaluated.

As in the Phase I test, the tunnel flow was effectively channeled into the exhaust duct model using a bell mouth at the model inlet. Various nozzle configurations were tested for performance, including two and three-nozzle deflector designs. A successful three nozzle arrangement is shown in Fig. 6. This three nozzle arrangement utilizes a momentum (no Coanda flow) nozzle along the upper wall, a semi-cylinder Coanda nozzle at the center of the exit plane, and a Coanda nozzle forming the lower wall lip. For the horizontal test arrangement, the exhaust deflection is downward.

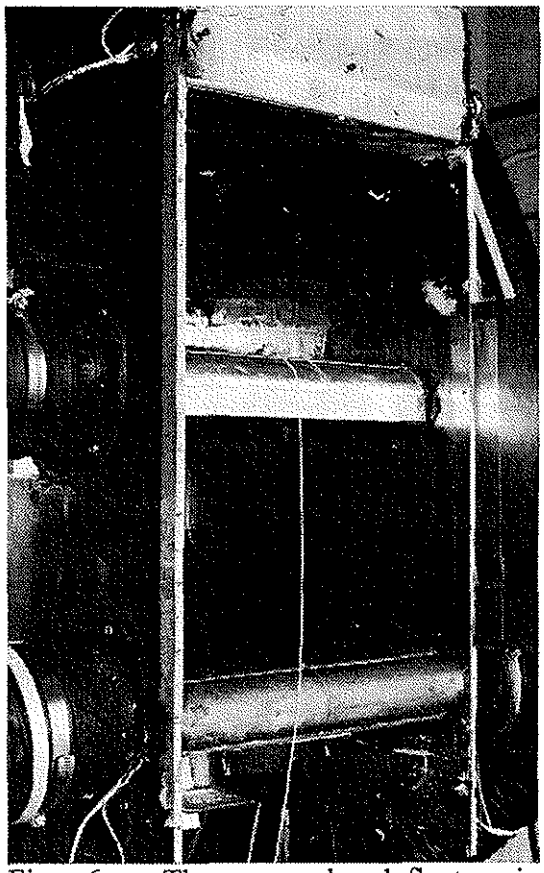

Fig. 6. Three nozzle deflector in simulated V-22 exhaust duct.

Nozzle air was provided by a high volume, low pressure centrifugal compressor rated at 6-PSIG at 1500 CFM which was well in excess of the requirements. To provide the desired flow rates, a single control valve was located upstream of a manifold which distributed the compressed air to each nozzle by means of flexible hoses. A general layout of the test module is presented in Fig. 7 which shows the two merging exhaust streams, and the locations of the nozzles.

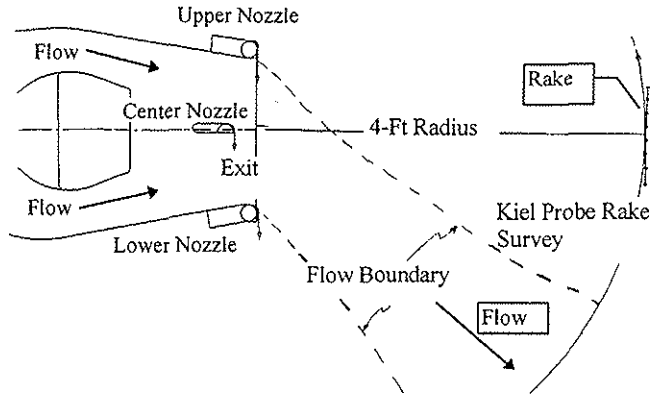

Fig. 7. V-22 exhaust model with deflector nozzles and wake rake survey location shown.

Nozzle flow parameters were determined from total pressure and temperature measurements taken from the air supply tubes just upstream of the each plenum. Pressure measurements indicated that losses were relatively small between the measurement location and the nozzle exit. Pressures were measured with a pitot probe and temperatures were obtained from a thermocouple readout.

The primary goal of this test was to evaluate performance for a given configuration by measuring the flow deflection angle for a given momentum coefficient. Flow deflection was determined by sweeping a Kiel probe rake through a constant radius arc

centered about the exit plane centerline (see Fig. 7). This wake momentum survey provided the flow magnitude at a given angular location relative to the axis of the tunnel. A weathercock vane device was also used to measure the actual flow angularity at the same radius and arc locations as the rake survey.

The Kiel probe rake was also used to survey the flow inside the duct (just upstream of the exit plane) so that the duct mass flow rate could be determined. The rake total pressures and the exit plane static pressure were recorded by computer so that the flow velocity distribution could be determined. Velocity, duct area and flow density were used to compute the duct momentum and mass flow rates for each test configuration. Separate pitot probes, located at representative locations in the duct, provided a secondary measure of the duct mass flow rate.

Phase II Test Data Reduction

During phase 2 testing the slot mass flow was determined from the measured flow conditions using isentropic flow relations for compressible flow. The expression for nozzle Mach number is determined by the ratio of the plenum pressure to the nozzle static pressure as given below:

$$M_{slot} = \sqrt{\left(\left(\frac{P_{o_{slot}}}{P_{exit}}\right)^{\frac{\gamma-1}{\gamma}} - 1\right) \cdot \frac{2}{\gamma - 1}}$$

For these tests it is assumed that the slot static pressure is equal to the duct exit plane pressure (approximately atmospheric). This involves an approximation for the Coanda nozzles, since the actual nozzle static pressure is slightly below atmospheric pressure, resulting in a slight under-prediction of slot Mach number. The static temperature of the slot air is determined by the isentropic relation:

$$T_{slot} = \frac{T_{o_{slot}}}{\left(1 + \frac{\gamma - 1}{2}\right) M_{slot}^{\ 2}}$$

Slot air density is determined from the ideal gas law as:

$$\rho_{slot} = \frac{P_{exit}}{R \cdot T_{slot}}$$

The nozzle mass flow may be determined as:

$$\dot{m}_{slot} = \rho_{slot} \cdot V_{slot} \cdot A_{slot}$$

where,

$$V_{slot} = M_{slot} \cdot a_{slot}$$

and,

$$a_{slot} = \sqrt{\gamma \cdot R \cdot T_{slot}}$$

The exhaust mass flow is determined by integrating the velocities derived from the Kiel probe rake survey (inside the duct) using the Bernoulli equation for incompressible flow. The distribution of velocity in the exhaust exit plane for the three nozzle configuration of Fig. 6. is depicted in Fig. 8. The velocity distribution is integrated to determine the mass flow exiting the duct while the

nozzles are active. For this run, the average exit plane velocity is 131 f/s.

The measured temperatures and pressures are used in the preceding equations to derive an operating C_μ of 0.037. The corresponding exhaust flow velocity distribution is presented in Fig. 9. The peak in velocity indicates that the flow has been deflected by approximately 40 degrees for this configuration. Thermo-vision camera flow visualization results corresponding to this configuration are shown in Fig. 10. Note that deflection is measured from horizontal since the undeflected wind tunnel flow (and duct exhaust) is horizontal.

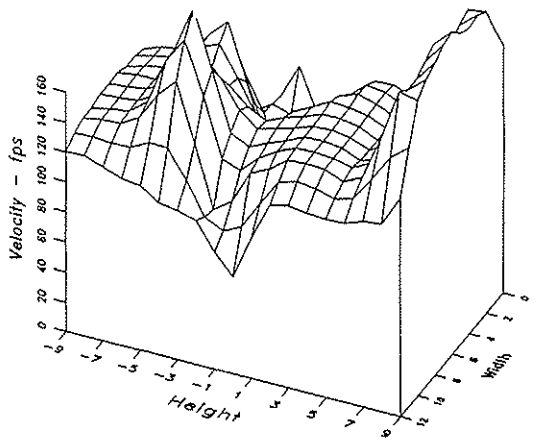

Fig. 8. Measured exit plane velocity distribution for three nozzle configuration.

The configuration discussed in Figs. 7. through 10 provided the maximum deflection for a given operating C_μ. In this configuration, the upper nozzle ejects a sheet of air at approximately 90 degrees to the ducted flow. Thus, the upper nozzle does not utilize the Coanda effect to redirect the flow. In effect, the upper nozzle acts like a jet flap. The center nozzle was positioned in the low velocity region produced by the center body. More flow deflection was achieved by positioning the center nozzle closer to the exit plane of the duct.

Two different nozzle configurations were tested at the center position. The first utilized a full cylinder Coanda effect nozzle with the slot air initially ejecting in the same direction as the duct flow. Testing with this nozzle revealed that the Coanda flow remained attached to the cylinder and eventually traveled upstream, back toward the center body. Consequently, the flow emerging from the lower half of the duct was mostly unaffected by this nozzle arrangement.

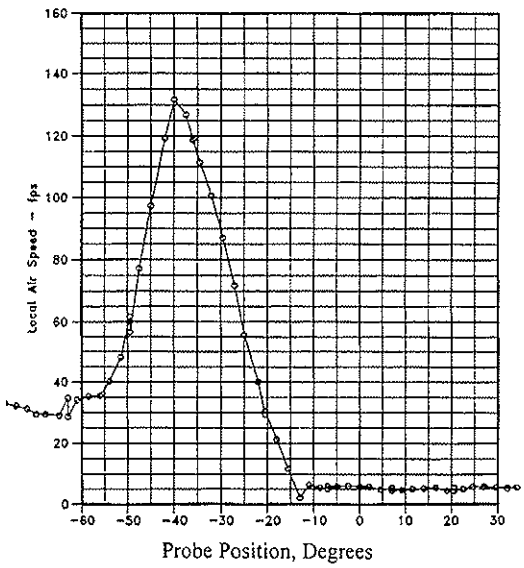

Fig. 9. Rake survey results for three nozzle deflector.

An improved center nozzle, utilizing a semi-cylinder design, was then tested. This design relied on the Coanda effect to "pull down" the flow from the upper side of the duct and used the momentum jet stream separating from the lower

edge of the semi-cylinder to deflect the lower stream of the duct flow.

Fig. 10. Exhaust plume for three-nozzle configuration indicates 40 degrees of deflection. (Flow from right to left.)

Test configurations for the lower nozzle included both full cylinder and semi-cylinder Coanda effect nozzles. The semi-cylinder lower nozzle did not improve the deflector performance, but was useful in forcing the slot flow to separate from the cylinder in a known direction. For the full cylinder lower nozzle, the slot flow was observed traveling upstream along the outside of the exhaust duct.

Increasing the cylinder diameter of the lower nozzle from 2 inches to 4 inches did not show any improvement in deflector performance. The Coanda flow did not stay attached to the 4 inch diameter cylinder as well as on the original 2 inch diameter cylinder. The reason is unclear, but may have to do with imperfections in that particular slot/cylinder design. In different runs, it was observed that the removal of some narrow spacers (used to maintain the slot gap) provided up to 10 degrees of additional flow deflection. Thus, the overall system performance depends strongly on designing a nozzle that provides uniform flow over the Coanda surface.

The effect of changing the lower Coanda nozzle slot height (with constant plenum back pressure) was also examined. In one run the lower nozzle slot height was doubled from 0.05 inch to 0.1 inch. In a following run the lower nozzle slot height was halved to 0.025 inches. For the same plenum operating pressures (and therefore the same slot velocities) the deflection data indicated essentially no change in deflection angle. Apparently the lower Coanda cylinder performance is dictated more by the velocity of the attached jet than the thickness of the jet. Although the derived values of C_μ for all testing configurations were within the ability of the V-22 bleed air limits, this result indicated that a smaller slot height with correspondingly lower mass flow can be applied on a Coanda nozzle without impairing the deflector performance.

Phase III V-22 Ground Test

The successful wind tunnel test program led to the selection of two configurations for ground testing on the V-22. The three nozzle arrangement of Fig. 7 was selected as the first test configuration but was designed with a removable center nozzle. The second configuration was obtained when the center nozzle was removed.

The slot height for each nozzle was fixed, and provided a total slot exit area slightly smaller than the total plenum hole area. The slot area formed the minimum area (choke point) of the bleed air passage. Thus, sonic flow conditions could be achieved at the slot for sufficiently large plenum back-pressure ratios.

The V-22 engine nacelle with the bleed air deflector system installed is shown in Fig. 11. In this configuration, the side walls of the exhaust duct are fixed. The bleed air is supplied from the 14th stage engine bleed air port and is routed along the outside of the nacelle to each of the three nozzles as seen in the figure. The bleed air flow is activated by an inline solenoid valve which is operated by the pilot. The bleed air tubing is external to the nacelle for testing purposes only. The deflector is instrumented with pressure transducers to measure the bleed air mass flow, temperature, line pressures, and plenum pressures.

Figure 12 shows the V-22 engine nacelle with a competing mechanical exhaust deflector design. An inboard flap and outboard exhaust duct wall are shown deployed to the operating position. The performance of each deflector unit was captured using a thermal imaging camera which recorded the exhaust plume heat radiation pattern during testing.

Testing was conducted at power settings ranging from 14% to 70% of maximum engine torque. The deflector system is intended for ground idle operations which include 100% rotor RPM and ± 3 deg collective settings. This corresponds to a low power setting near 14% engine torque. Higher torque conditions were tested to evaluate deflector performance for off-design conditions. Testing at higher power settings demonstrated that the bleed air deflector performance was approximately independent of power setting. Each increase in power results in an increased exhaust mass flow which is balanced by a corresponding increase in total nozzle mass flow. As engine power increases, the bleed air supply pressure increases, and an approximately constant ratio of bleed air to exhaust air mass flow is maintained without requiring a bleed air supply throttle.

During the test program the two nozzle deflector system was shown to be as effective in deflecting the exhaust flow as the competing mechanical deflector design. The three nozzle bleed air deflector provided the most deflection and the lowest corresponding fuselage temperature environment. However, the two nozzle deflector (which eliminated the center nozzle) provided adequate temperature reductions at the fuselage, and eliminated approximately 30% of the weight and cost of the three nozzle design.

Thermal imaging results for the bleed air and mechanical deflector are shown in Figs. 13-14. Figure 13 shows a frontal view of the V-22 right hand nacelle with the bleed air deflector installed. The camera position for this view is the same for the thermal imaging camera views of Figs. 14a, b. The exhaust visualization shown in Figs 14 a and b compare the exhaust plumes for the two nozzle bleed air deflector and the mechanical deflector. These results indicate that the

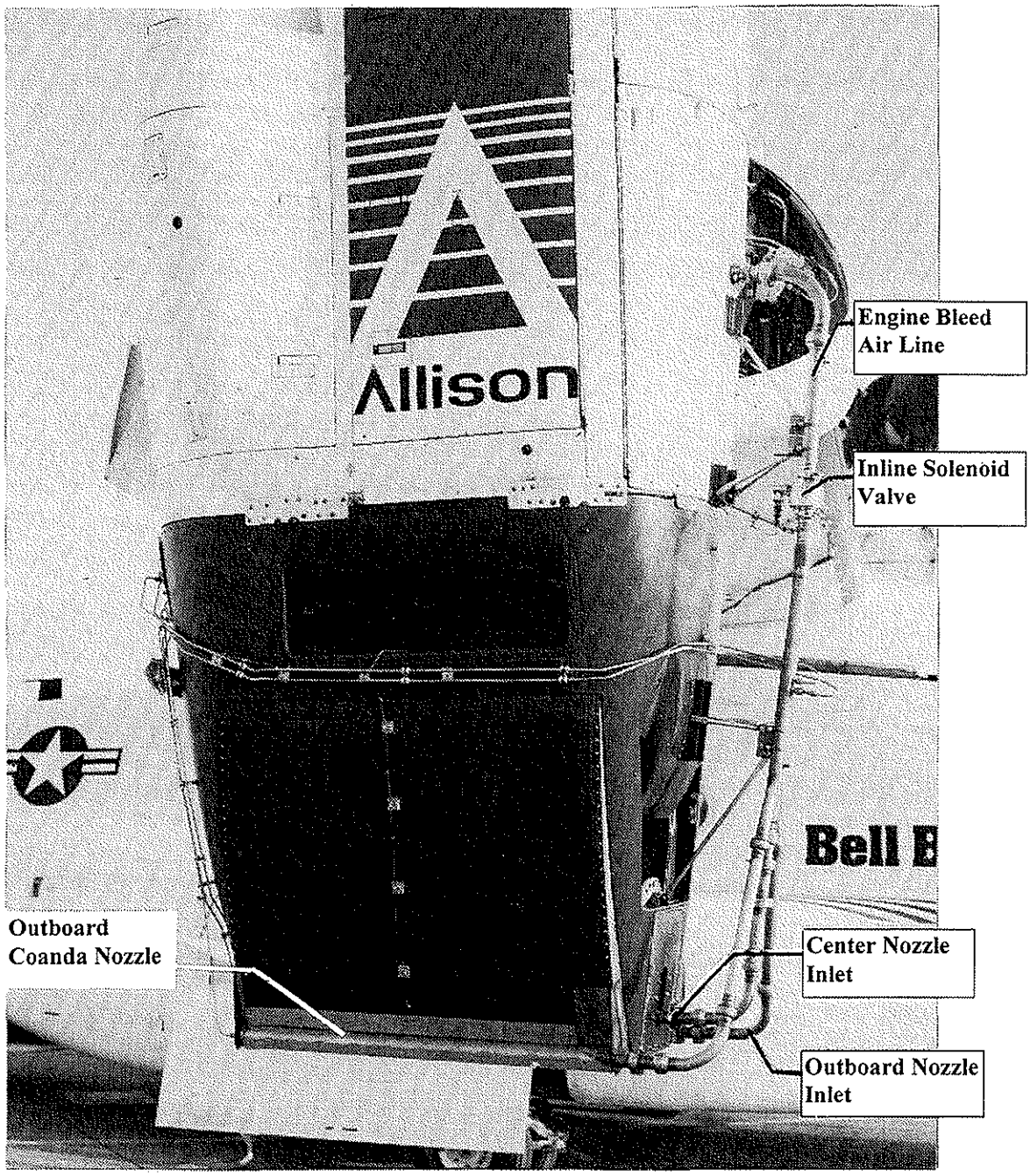

Fig. 11. V-22 nacelle with Coanda effect exhaust deflector installed.

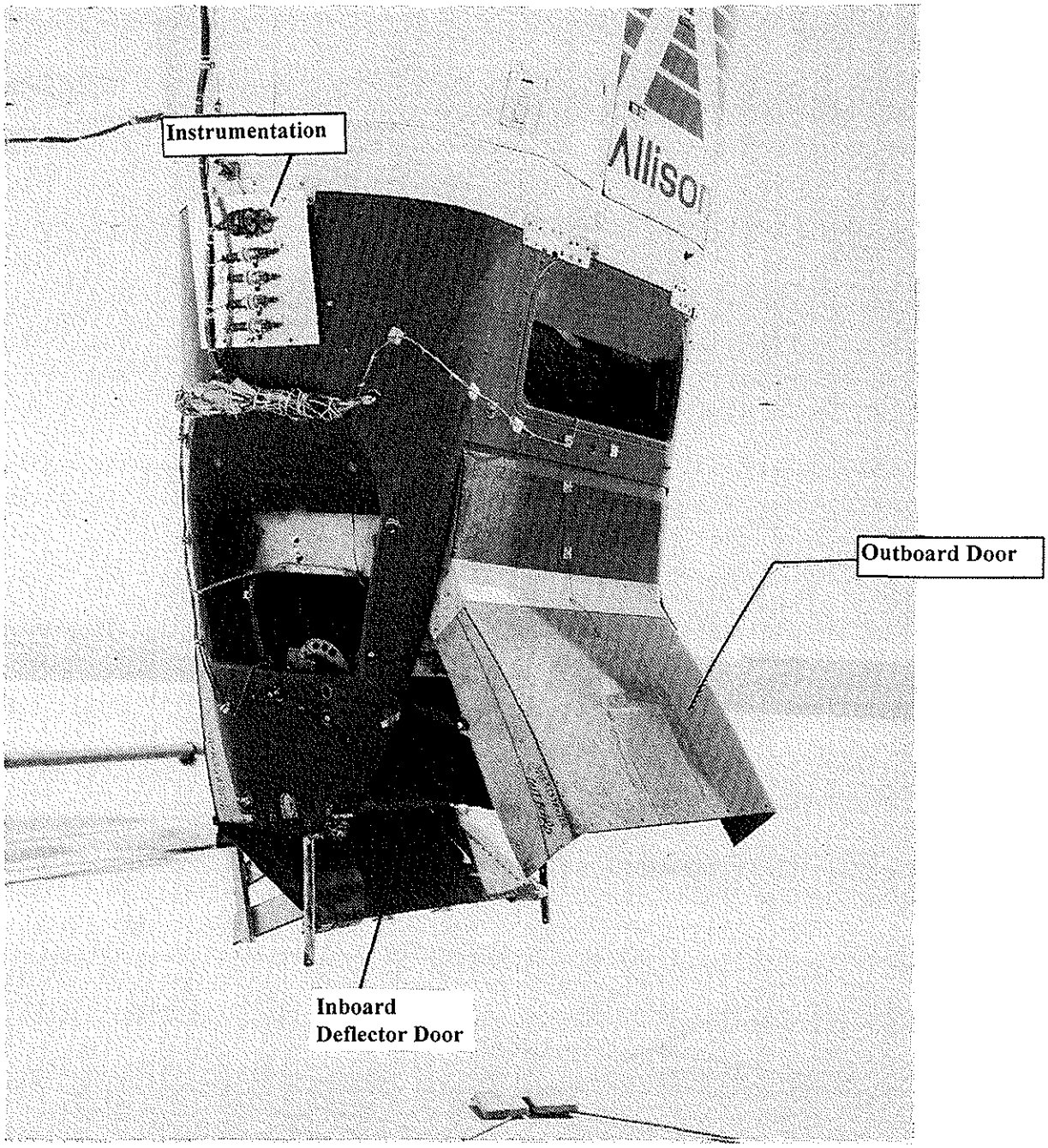

Fig. 12 V-22 nacelle with mechanical exhaust deflector test article

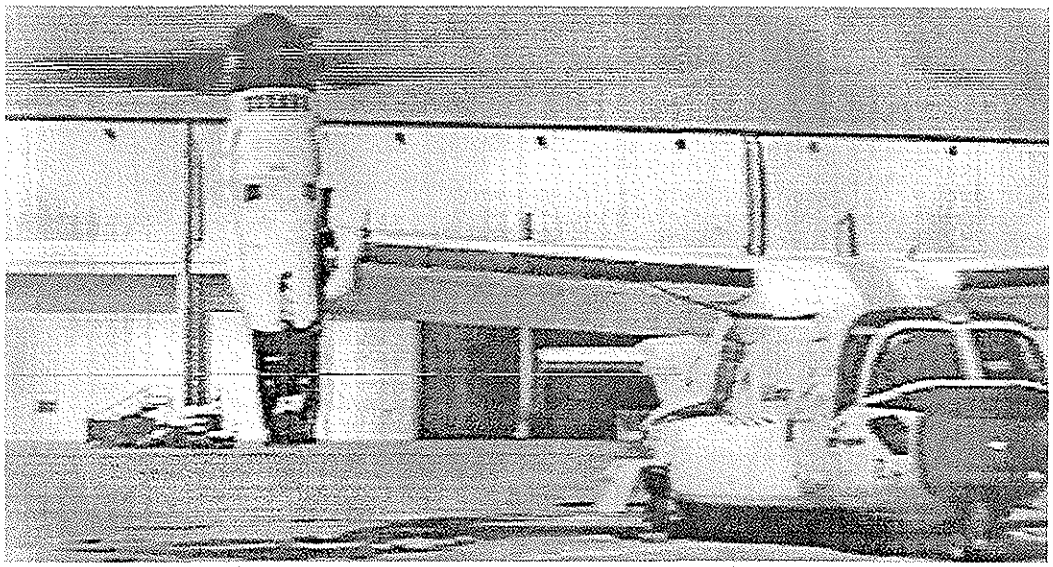

Fig. 13 V-22 nacelle and exhaust with Coanda deflector installed.

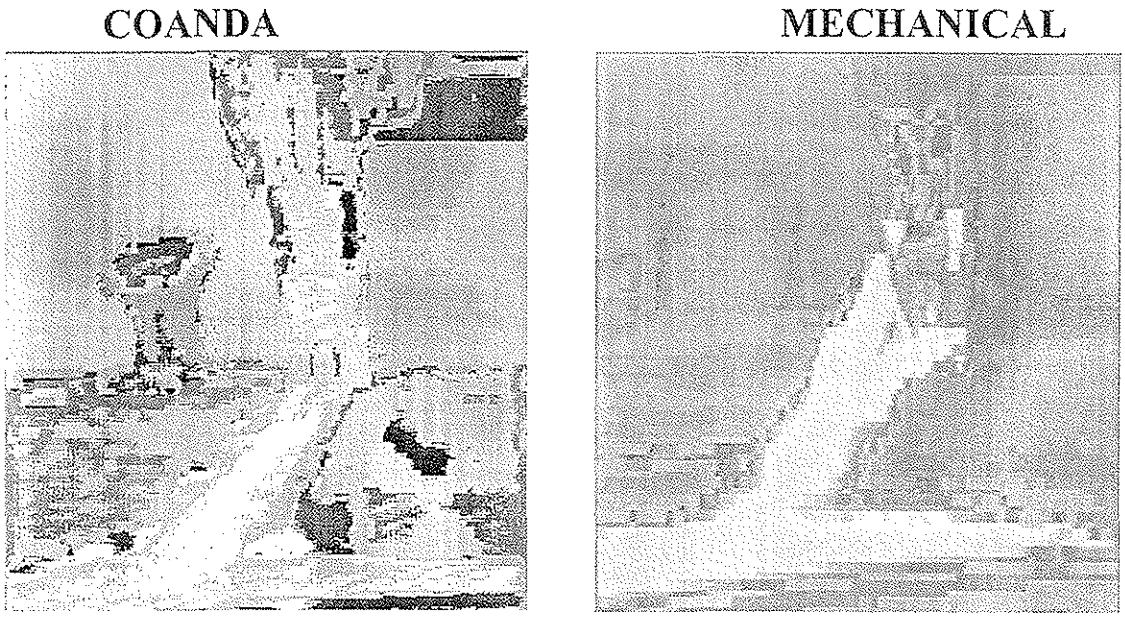

Fig. 14 Comparison of exhaust flow for the two nozzle Coanda deflector (a) and Mechanical deflector (b) as seen with thermo-vision camera.

two nozzle bleed air deflector system matches the deflection capability of the competing mechanical deflector design. Secondary thermocouple readings showed that fuselage temperatures for the two-nozzle bleed air deflector were lower than the mechanical deflector design.

Total pressure measured in the bleed air supply line varied from 73 PSIA at low power to 124 PSIA at high power settings. Flow at the nozzle slots also varied with power setting and the Mach number ranged from high subsonic to sonic conditions, based on plenum pressure measurements. Data reduction from the two nozzle deflector test indicated that the system utilized between 5.9 % and 7.3 % of the engine bleed air through the range of power settings, while deflecting the exhaust by approximately 45 degrees. Thus, the primary goal of limiting bleed air utilization to less than 7% during ground idle operations was achieved.

Conclusions

A bleed air exhaust deflector system was developed for the V-22. Both a two and a three nozzle design were tested against a competing mechanical deflector. Ground test results on the V-22 aircraft showed that both bleed air systems provided a cooler temperature environment for the aircraft than the mechanical system. V-22 ground tests verified the results obtained during wind tunnel testing.

For each deflector system tested on the V-22, exhaust gas deflections in excess of 40 degrees were obtained. The three nozzle deflector provided the most deflection and the lowest fuselage temperatures. Measured results showed that the center nozzle of this bleed air deflector could be eliminated and still provide adequate exhaust deflection. The resulting two nozzle system utilizes a momentum jet nozzle on the inboard nacelle wall and a Coanda effect nozzle on the outboard nacelle wall to deflect exhaust gases outboard, away from the fuselage.

Trade studies of the bleed air deflector system determined that both cost and weight savings could be realized for the V-22 aircraft by using the two-nozzle design instead of the mechanical deflector option. The cost and weight savings are the result of eliminating hinges, actuators, and all moving parts on the nacelle. These parts are replaced by lightweight bleed air supply tubing, an inline solenoid valve, and the inboard and outboard nozzles. The cost and weight savings has led to the Navy's selection of the two nozzle bleed air deflector for incorporation into the EMD aircraft.

Acknowledgments

The authors would like to thank the Bell Helicopter Research Lab team for their assistance in conducting the experiments. Mr. Brent Achttien constructed the Phase 1 wind tunnel model and assisted in the initial testing. Mr. Ralph Rockett constructed most of the parts used in the Phase 2 test program and provided many useful suggestions to simplify the test program. Mr. Martin Peryea developed the data acquisition systems for the Phase 2 wind tunnel test. His assistance during testing is also gratefully acknowledged. The

helpful suggestions of Mr. Dale Sowers throughout the Phase 2 testing and his support during V-22 ground tests is greatly appreciated. The authors also acknowledge the funding and support of the Phase 2 and 3 test program by the US Navy.

References

1) Henri Coanda, "Device for Deflecting a Stream of Elastic Fluid Projecting into an Elastic Fluid," United States Patent Number 2,052,869, September 1, 1936.

2) R.J. Englar, M.J. Smith, S.M. Kelly and R.C. Rover III, "Development of Circulation Control Technology for Application to Advanced Subsonic Transport Aircraft, AIAA Paper 93-0644, 31st Aerospace Sciences Meeting and Exhibit, Reno, Nevada, January 11-14, 1993.

3) K.R. Reader and W.J. Dixon, J.R., "Evaluation of a Ten Foot Diameter X-Wing Rotor," Proceedings of the 40th Annual Forum of the American Helicopter Society, Washington, D.C., May 16-18, 1984, pp. 377-387

4) A.L. Winn and A.H. Logan, "The MDHC NOTAR System," Proceedings of The Helicopter Yaw Control Concepts Conference of The Royal Aeronautical Society, Feb. 28-March 1, 1990

5) Englar, R.J., "Two-Dimensional Subsonic Wind Tunnel Investigations of a Cambered 30-Percent Thick Circulation Control Airfoil," David Taylor Naval Ship Research and Development Center, Technical Note AL-201, May 1972.

6) Englar, R.J., "Experimental Investigation of the High Velocity Coanda Wall Jet Applied to Bluff Trailing Edge Circulation Control Airfoils," David Taylor Naval Ship Research and Development Center, Technical Note AL-308, June 1973.